Deep inverse Radar Models as Priors for evidential Occupancy Mapping

Tiefe inverse Radarmodelle as A-priori-Information in evidenzbasierten Belegungskarten

Der Fakultät für Maschinenwesen der Rheinisch-Westfälischen Technischen Hochschule Aachen vorgelegte Dissertation zur Erlangung des akademischen Grades eines Doktors der Ingenieurwissenschaften

Daniel Bauer

IMPRESSUM

WIRD VOM INSTITUT GESTALTET

Preface

Der Fakultät für Maschinenwesen der Rheinisch-Westfälischen Technischen Hochschule Aachen vorgelegte Dissertation zur Erlangung des akademischen Grades eines Doktors der Ingenieurwissenschaften

Hier eventuell eigenen Text.

Aachen, im Januar 2033

Max Mustermann

Contents

1 Deep, evidential ISMs as Priors for Occupancy Mapping Experiments

1.1 Experiment to verify Choices of Combination Rules

In this section, a qualitative verification of the combination rules' properties derived in Sec. **??** is provided. To demonstrate the properties, an evidential occupancy signal (first row Fig. 1-1) is fused over time with a mass initialized with $m_u = 1$ using different combination rules. The signal starts with a step-wise ramp-up of the occupied mass, followed by a completely contradictory signal, a signal with partial conflict, the consecutive contradicting signals and, eventually, a signal with full conflict.

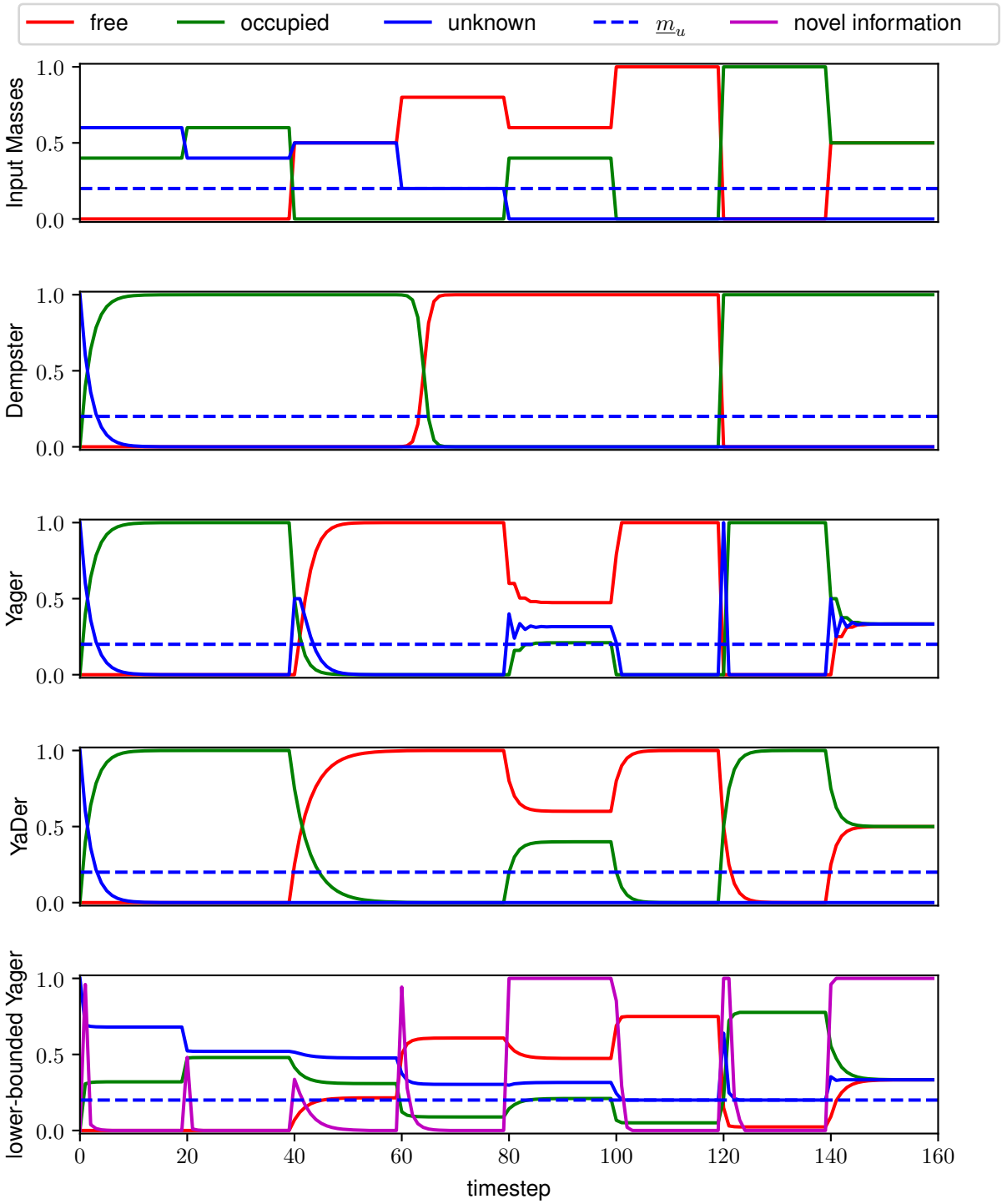

Fig. 1-1: This figure shows the qualitative evaluation of the different evidential combination rules given input signals for free, occupied and unknown mass (first subplot) over time with an exemplary lower unknown threshold $\underline{m}_u$ overlayed.

Beginning with Dempster's rule, it can be seen that the fused mass always fully converges to the class of the signal with the highest portion (see Dempster graph e.g. in the time interval $[0, 20]$). Given temporal independent information and no conflict, this behavior would be desired since each time step provides new evidence of the state. However, in presence of conflict, the fused mass should converge to a state representing the portion of conflict to represent cells being dynamic. Since Dempster's rule lacks the ability to do so, it is disqualified for usage in this work.

Similar to Dempster's rule, Yager's rule, in absence of conflict, converges fully to the dominating class (see Yager graph e.g. in the time interval $[0, 20]$). In presence of conflicting mass, Yager's rule recuperates unknown mass (see e.g. time interval $[35, 45]$) and allows to directly switch the state, as opposed to Dempster's rule (compare Dempster and Yager graph in time interval $[35, 45]$). The recuperation capability is useful in the initialization phase to correct for state changes without falling below $\underline{m}_u$. Also, while Yager's rule is capable of representing the conflict state of a signal (see Yager graph in the time interval $[80, 100]$ and $[140, 160]$) it never reaches the original input conflict due to the recuperated unknown mass. It shall be argued that the property of recuperating unknown mass outweighs the deficit of biased conflict representation for the purpose of initializing the occupancy state.

To solve the biased conflict state in the convergence phase, the YaDer rule has been proposed. It can be seen that by equally distributing the conflict into the conflicting classes instead of shifting it to the unknown class, the fused mass converges to the input's conflict state (see YaDer graph in the time interval $[80, 100]$ and $[140, 160]$). Also, in case of absent conflict, YaDer rule, like Yager and Dempster, fully converges to the dominating class (see YaDer graph e.g. in the time interval $[0, 20]$). Thus, the YaDer rule combines both the Yager rule's property to represent conflict and Dempster rule's property to strictly reduce the unknown mass, giving it its name. These properties makes YaDer rule an ideal candidate to be used in the convergence phase.

Eventually, the lower-bounded (lb) Yager rule's property to only converge to the input signal until the same unknown mass is reached is shown in the last graph (e.g. in time interval $[0, 30]$). It can be seen that there is a discrepancy between the converged fused state and the input mass. This is due to the fact that the input is assumed to originate from a deep Inverse Sensor Model (ISM) with limited certainty. Therefore, the input is first rescaled into the interval $m_u \in [\underline{m}_u, 1]$ before fed into the lb Yager rule. Moreover, it can be seen when comparing the time intervals $[35, 45]$ and $[45, 55]$ that a state switch between free and occupied can only be realized if the conflicting signal has high enough certainty relative to the current state. This is desired in order not to overwrite a highly certain estimate, potentially predicted close to data, with lower certain ones, potentially based on extrapolations. Problematic, however, is that the state change is not fully completed letting the fused mass converge to a conflicting state. This is due to in-

creasingly discounting the input signal when reducing the difference in unknown mass between input and fused signal. This property ensures that once $\underline{m_u}$ is reached, the deep ISM can not further influence the fused mass (see lower-bounded Yager graph in the time interval $[100, 160]$). Here, it shall argued that the benefit of reducing the influence of outliers and the property of deactivating the deep ISM's influence outweigh the shortcoming of incomplete state change for the initialization phase.

1.2 Analysis of redundant Information in Deep ISMs

1.2.1 Setup of Redundancy Analysis in Deep ISMs

To verify , occupancy maps are created in four ways. The baseline is the direct accumulation using Yager's rule, abbreviated as "accum.". This is evaluated for the deep as well as the geo ISM. Second, a naive solution is evaluated which moves all free and occupied mass to unknown for predictions with $m_u >= 0.9$ to hinder small predictions to accumulate over time ("accum. with cutoff"). Third, the method as proposed in is used to reduce the redundancy ("accum. with redundancy reduction"). Eventually, the fusion using the deep and geo ISMs by directly accumulating the predictions with Yager's rule is evaluated ("accum. fusion"). Here, the fusion is investigated to analyze whether the deep ISM indeed overwrites most of the geo ISM's predictions as proposed in . The evaluation is performed using only the accumulated radar detections of the recent 20 timesteps (R_{20}) since the focus of this work lies on radar occupancy mapping. Additionally, it is assumed that the effects are similar using other sensor modalities. The geo ISM method is used as described in and ShiftNet, as described , is used as a deep ISM. The metrics used are the normed confusion matrix and the mIoU . Here, the metrics are evaluated separately in all of the area in a 20m vicinity around the ego vehicle trajectory ("whole mapped area") and in an area of 15 pixels around occupied ground truth pixels in the reference occupancy maps. Here, the mIoU is only evaluated around the occupied borders to quantify the cleanliness. The reference maps are created by accumulating the geo ILM. Two examples of the evaluation areas can be found in 1-3. The scenes mapped are solely taken from the test set which was not used during training.

Hypothesis bla

section or equation

Hypothesis bla

ref to geo ISM

ref to ShiftNet

ref to conf matrix definition

ref to mIoU definition

1.2.2 Results of Redundancy Analysis in Deep ISMs

- show alleys for both mapping methods

- show mapping progress that illustrates the overwriting of correct assignments

	k	f	o	u	f	o	u
geo $IR_{20}M$ accumulated	$p(k\|f)$	57.9	2.3	39.8	44.3	5.9	49.8
	$p(k\|o)$	16.1	36.3	47.6	15.9	36.0	48.1
	$p(k\|u)$	2.8	5.7	91.5	4.0	9.7	86.3
	mIoU	-	-	-	16.8	24.6	14.2
deep $IR_{20}M$ accumulated	$p(k\|f)$	86.6	11.7	1.7	68.2	28.4	3.4
	$p(k\|o)$	27.2	69.6	3.2	27.3	69.4	3.3
	$p(k\|u)$	28.9	57.5	13.6	27.2	64.5	8.3
	mIoU	-	-	-	15.3	12.4	2.8
deep $IR_{20}M$ accumulated with cutoff	$p(k\|f)$	87.4	10.5	2.1	69.4	26.7	3.9
	$p(k\|o)$	28.3	67.0	4.7	28.4	66.8	4.8
	$p(k\|u)$	33.7	34.7	31.6	30.4	51.9	17.7
	mIoU	-	-	-	15.1	16.5	5.2
deep & geo $IR_{20}M$ accumulated fusion	$p(k\|f)$	86.7	11.6	1.7	68.4	28.3	3.3
	$p(k\|o)$	27.3	69.5	3.2	27.4	69.3	3.3
	$p(k\|u)$	29.0	57.4	13.6	27.3	64.4	8.3
	mIoU	-	-	-	15.3	12.4	2.7
deep $IR_{20}M$ accumulated with redundancy reduction	$p(k\|f)$	88.5	5.9	5.6	71.6	16.7	11.7
	$p(k\|o)$	29.0	55.7	15.3	29.0	55.4	15.6
	$p(k\|u)$	26.3	12.9	60.8	26.3	23.4	50.3
	mIoU	-	-	-	16.8	23.4	11.8
		whole mapped area			boundary area		

Fig. 1-2: Normed confusion matrix for the three mapping variants using deep ISMs based on ShiftNet applied on different sensor modalities. See 1.2.1 for further information on the methods and abbreviations used.

Fig. 1-2 shows that, even though, the geo $IR_{20}M$'s occupancy map has the least true positive rates overall, it also has by far the least false rates. This is most significant when comparing its occupied false rate with the deep $IR_{20}M$ maps. Here, the deep $IR_{20}Ms$ without redundancy reduction produce about five times and the one with the reduction about twice the amount of false occupied predictions in the whole mapped area.

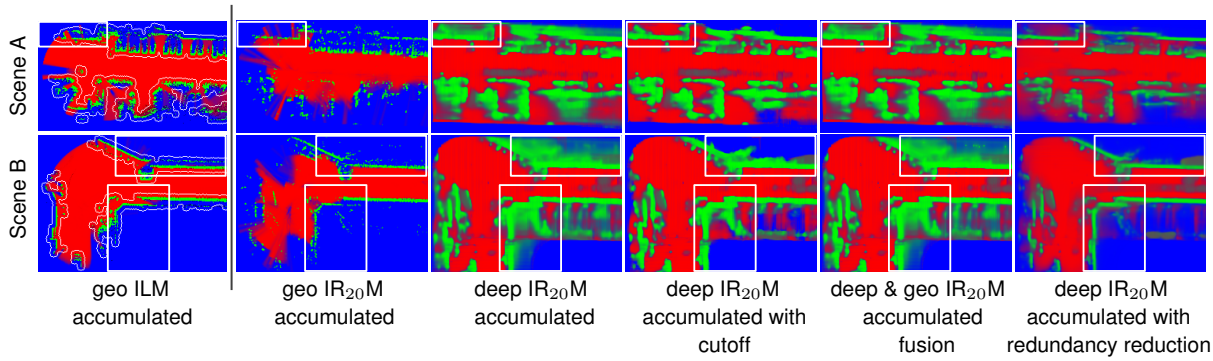

Fig. 1-3: Qualitative results of the three mapping approaches using different sensor modalities for two scenes. Here, the first row shows the ground truth map created by accumulating the geo ILM with the evaluation area overlayed in white around the occupied pixels. The other maps are created using deep ISMs based on ShiftNet with there respective sensor inputs (see Sec. 1.2.1).

Discussion

1.3 Analysis of Deep ISM Priors for Occupancy Mapping

Setup

Experiment

	k \	f	o	u	f	o	u	f	o	u
geo IR$_{20}$M	$p(k\|f)$	59.9	8.1	32.0	100.0	0.0	0.0	0.0	20.9	79.1
accumulated	$p(k\|o)$	21.7	50.1	28.2	0.0	100.0	0.0	42.7	0.0	57.3
	$p(k\|u)$	11.1	33.7	55.2	0.0	0.0	100.0	25.6	74.4	0.0
deep & geo IR$_{20}$M	$p(k\|f)$	78.3	16.7	5.0	88.1	9.3	2.6	63.1	28.4	8.5
accumulated	$p(k\|o)$	29.2	65.1	5.7	8.3	89.8	1.9	47.9	42.4	9.7
fusion	$p(k\|u)$	33.4	48.9	17.7	41.0	29.8	29.2	23.6	73.2	3.2
deep & geo IR$_{20}$M	$p(k\|f)$	77.8	13.0	9.2	91.4	6.0	2.6	57.0	24.1	18.9
accumulated	$p(k\|o)$	26.2	63.5	10.3	5.2	92.5	2.3	47.8	33.2	19.0
...	$p(k\|u)$	27.8	43.0	29.2	31.5	18.8	49.7	23.2	73.2	3.6
ShiftNet		geo IR$_{20}$M$(m_u) < 1$			geo IR$_{20}$M$(m_u) < 1$ & correct			geo IR$_{20}$M$(m_u) < 1$ & false		

Fig. 1-4:

The table distinguishes between areas touched and untouched ($m_u = 1$) by the original geo IRM which where still inside an area of 20m around the ego vehicles trajectory (see for an example of the mapped area). Thus, the majority of the so called untouched areas lies at the borders of the mapped area.

Fig

	deep $IR_{20}M$	deep IDM	deep $IDR_{20}M$
p(fused Map(m_u < 0.300) | geo IRM Map(m_u = 1), $\underline{m}_u$=0.3)	0.00023%	0.00026%	0.00043%
#(fused Map(m_u < 0.300) | geo IRM Map(m_u = 1), $\underline{m}_u$=0.3)	2476	2735	4613
#(fused Map(m_u < 0.298) | geo IRM Map(m_u = 1), $\underline{m}_u$=0.3)	0	0	0

Fig. 1-5: Analysis of how often the lower bound on the unknown mass $\underline{m}_u$ has been violated in the fused map in areas where the geo IRM has not been active. The violations are given in percentage and absolute. Also, the amount of violations given some slack on the condition are provided.

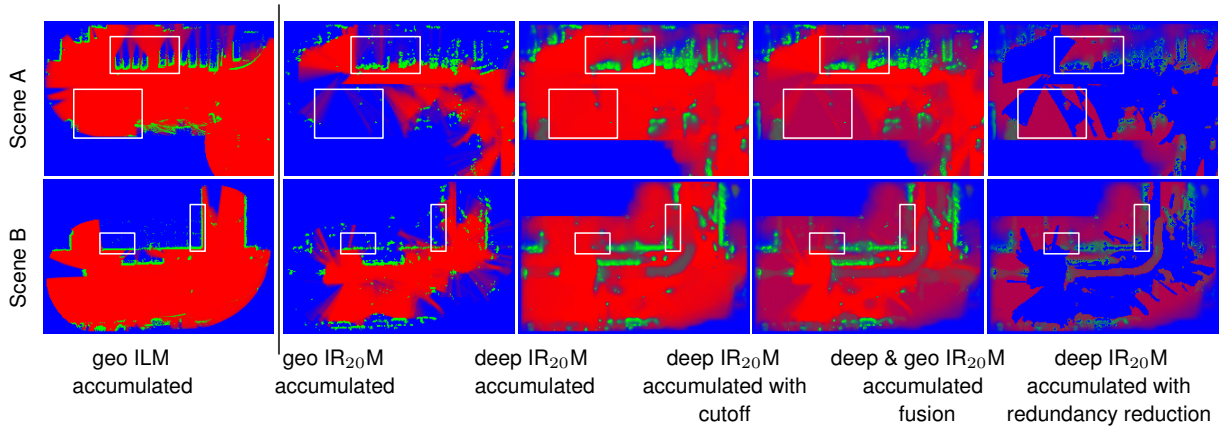

Fig. 1-6: Qualitative results of the three mapping approaches using different sensor modalities for two scenes. Here, the first row shows the ground truth map created by accumulating the geo ILM with the evaluation area overlayed in white around the occupied pixels. The other maps are created using deep ISMs based on ShiftNet with there respective sensor inputs (see Sec. 1.2.1).

Qualitative results

- upper white box in scene A: wrong extrapolation
- lower white box in scene A: shortcoming of geo $IR_{20}M$ can be compensated by initializing those areas using the deep $IR_{20}M$
- both white boxes in scene B: errors in deep $IR_{20}M$ don't converge to certainty (see image of initialized areas). Geo $IR_{20}M$ keeps them in check... or something like that.

Discussion

2 Bibliography

[ABA16] ABADI, M., BARHAM, P., CHEN, J., CHEN, Z., DAVIS, A., DEAN, J., DEVIN, M., GHEMAWAT, S., IRVING, G., ISARD, M., et al.
Tensorflow: A system for large-scale machine learning
12th {USENIX} Symposium on Operating Systems Design and Implementation ({OSDI} 16), 2016, pp. 265–283

[ASV15] ASVADI, A., PEIXOTO, P., NUNES, U.
Detection and tracking of moving objects using 2.5 d motion grids
2015 IEEE 18th International Conference on Intelligent Transportation Systems, IEEE, 2015, pp. 788–793

[BAZ18] BAZAREVSKY, V., TKACHENKA, A.
Mobile Real-time Video Segmentation
Google AI Blog (2018)

[BEN09] BENESTY, J., CHEN, J., HUANG, Y., COHEN, I.
Pearson correlation coefficient
Noise reduction in speech processing, Springer, 2009, pp. 1–4

[BER18] BERMAN, M., RANNEN TRIKI, A., BLASCHKO, M. B.
The lovász-softmax loss: A tractable surrogate for the optimization of the intersection-over-union measure in neural networks
Proceedings of the IEEE Conference on Computer Vision and Pattern Recognition, 2018, pp. 4413–4421

[CAE20] CAESAR, H., BANKITI, V., LANG, A. H., VORA, S., LIONG, V. E., XU, Q., KRISHNAN, A., PAN, Y., BALDAN, G., BEIJBOM, O.
nuscenes: A multimodal dataset for autonomous driving
Proceedings of the IEEE/CVF Conference on Computer Vision and Pattern Recognition, 2020, pp. 11621–11631

[CAO17] CAO, Y., WU, Z., SHEN, C.
Estimating depth from monocular images as classification using deep fully convolutional residual networks
IEEE Transactions on Circuits and Systems for Video Technology 28.11 (2017), pp. 3174–3182

[CAR15] CARRILLO, H., DAMES, P., KUMAR, V., CASTELLANOS, J. A.
Autonomous robotic exploration using occupancy grid maps and graph slam based on shannon and rényi entropy
2015 IEEE international conference on robotics and automation (ICRA), IEEE, 2015, pp. 487–494

[CAT11] CATTANEO, M. E.
Belief functions combination without the assumption of independence of the information sources
International Journal of Approximate Reasoning 52.3 (2011), pp. 299–315

[CHE18] CHEN, L.-C., ZHU, Y., PAPANDREOU, G., SCHROFF, F., ADAM, H.
Encoder-Decoder with Atrous Separable Convolution for Semantic Image Segmentation
ECCV, 2018

[CHO17] CHOLLET, F.
Xception: Deep learning with depthwise separable convolutions
Proceedings of the IEEE conference on computer vision and pattern recognition, 2017, pp. 1251–1258

[CLA12] CLARKE, B., WORRALL, S., BROOKER, G., NEBOT, E.
Sensor modelling for radar-based occupancy mapping
2012 IEEE/RSJ International Conference on Intelligent Robots and Systems, IEEE, 2012, pp. 3047–3054

[COR16] CORDTS, M., OMRAN, M., RAMOS, S., REHFELD, T., ENZWEILER, M., BENENSON, R., FRANKE, U., ROTH, S., SCHIELE, B.
The cityscapes dataset for semantic urban scene understanding
Proceedings of the IEEE conference on computer vision and pattern recognition, 2016, pp. 3213–3223

[DAV07] DAVISON, A. J., REID, I. D., MOLTON, N. D., STASSE, O.
MonoSLAM: Real-time single camera SLAM
IEEE transactions on pattern analysis and machine intelligence 29.6 (2007), pp. 1052–1067

[DEM68] DEMPSTER, A. P.
A generalization of Bayesian inference
Journal of the Royal Statistical Society: Series B (Methodological) 30.2 (1968), pp. 205–232

[DIN02] DING, J., WANG, W.-s., ZHAO, Y.-l.
General correlation coefficient between variables based on mutual information
JOURNAL-SICHUAN UNIVERSITY ENGINEERING SCIENCE EDITION 34.3 (2002), pp. 1–5

[EIG14] EIGEN, D., PUHRSCH, C., FERGUS, R.
Depth map prediction from a single image using a multi-scale deep network
Advances in neural information processing systems 27 (2014), pp. 2366–2374

[ELF89] ELFES, A.
Using occupancy grids for mobile robot perception and navigation
Computer 22.6 (1989), pp. 46–57

[FEN19] FENG, D., ROSENBAUM, L., TIMM, F., DIETMAYER, K.
Leveraging heteroscedastic aleatoric uncertainties for robust real-time lidar 3d object detection

2019 IEEE Intelligent Vehicles Symposium (IV), IEEE, 2019, pp. 1280–1287

[FIS81] FISCHLER, M. A., BOLLES, R. C.
Random sample consensus: a paradigm for model fitting with applications to image analysis and automated cartography
Communications of the ACM 24.6 (1981), pp. 381–395

[FLE07] FLEURET, F., BERCLAZ, J., LENGAGNE, R., FUA, P.
Multicamera people tracking with a probabilistic occupancy map
IEEE transactions on pattern analysis and machine intelligence 30.2 (2007), pp. 267–282

[FU18] FU, H., GONG, M., WANG, C., BATMANGHELICH, K., TAO, D.
Deep ordinal regression network for monocular depth estimation
Proceedings of the IEEE Conference on Computer Vision and Pattern Recognition, 2018, pp. 2002–2011

[GAR16] GARG, R., BG, V. K., CARNEIRO, G., REID, I.
Unsupervised cnn for single view depth estimation: Geometry to the rescue
European conference on computer vision, Springer, 2016, pp. 740–756

[GEI13] GEIGER, A., LENZ, P., STILLER, C., URTASUN, R.
Vision meets robotics: The kitti dataset
The International Journal of Robotics Research 32.11 (2013), pp. 1231–1237

[GOD17] GODARD, C., MAC AODHA, O., BROSTOW, G. J.
Unsupervised monocular depth estimation with left-right consistency
Proceedings of the IEEE Conference on Computer Vision and Pattern Recognition, 2017, pp. 270–279

[GOD19] GODARD, C., MAC AODHA, O., FIRMAN, M., BROSTOW, G. J.
Digging into self-supervised monocular depth estimation
Proceedings of the IEEE international conference on computer vision, 2019, pp. 3828–3838

[GOO16] GOODFELLOW, I., BENGIO, Y., COURVILLE, A., BENGIO, Y.
Deep learning
Vol. 1, 2, MIT press Cambridge, 2016

[GOO20] GOODFELLOW, I., POUGET-ABADIE, J., MIRZA, M., XU, B., WARDE-FARLEY, D., OZAIR, S., COURVILLE, A., BENGIO, Y.
Generative adversarial networks
Communications of the ACM 63.11 (2020), pp. 139–144

[GUI20] GUIZILINI, V., LI, J., AMBRUS, R., PILLAI, S., GAIDON, A.
Robust Semi-Supervised Monocular Depth Estimation With Reprojected Distances
Conference on Robot Learning, PMLR, 2020, pp. 503–512

[GUO11] GUO, C., SATO, W., HAN, L., MITA, S., MCALLESTER, D.
Graph-based 2D road representation of 3D point clouds for intelligent vehicles
2011 IEEE Intelligent Vehicles Symposium (IV), IEEE, 2011, pp. 715–721

[GUR06] GURALNIK, V., MYLARASWAMY, D., VOGES, H.
On handling dependent evidence and multiple faults in knowledge fusion for engine health management
2006 IEEE aerospace conference, IEEE, 2006, 9–pp

[HAK08] HAKLAY, M., WEBER, P.
Openstreetmap: User-generated street maps
IEEE Pervasive Computing 7.4 (2008), pp. 12–18

[HAN08] HAN, D., HAN, C., YANG, Y.
A modified evidence combination approach based on ambiguity measure
2008 11th International Conference on Information Fusion, IEEE, 2008, pp. 1–6

[21] HDL-32R
Velodyne Lidar, 2021, URL: https://velodynelidar.com/products/hdl-32e/

[HE15] HE, K., ZHANG, X., REN, S., SUN, J.
Delving deep into rectifiers: Surpassing human-level performance on imagenet classification
Proceedings of the IEEE international conference on computer vision, 2015, pp. 1026–1034

[HE16] HE, K., ZHANG, X., REN, S., SUN, J.
Deep residual learning for image recognition
Proceedings of the IEEE conference on computer vision and pattern recognition, 2016, pp. 770–778

[HEN20] HENDY, N., SLOAN, C., TIAN, F., DUAN, P., CHARCHUT, N., XIE, Y., WANG, C., PHILBIN, J.
FISHING Net: Future Inference of Semantic Heatmaps In Grids
arXiv preprint arXiv:2006.09917 (2020)

[HOR91] HORNIK, K.
Approximation capabilities of multilayer feedforward networks
Neural networks 4.2 (1991), pp. 251–257

[HOU62] HOUGH, P. V.
Method and means for recognizing complex patterns
US Patent 3,069,654, Dec. 1962

[JAD15] JADERBERG, M., SIMONYAN, K., ZISSERMAN, A., et al.
Spatial transformer networks
Advances in neural information processing systems 28 (2015), pp. 2017–2025

[JIA09] JIANG, H.-N., XU, X.-B., WEN, C.-L.
The combination method for dependent evidence and its application for simultaneous faults diagnosis
2009 International Conference on Wavelet Analysis and Pattern Recognition, IEEE, 2009, pp. 496–501

[JIN19] JING, Y., YANG, Y., FENG, Z., YE, J., YU, Y., SONG, M.
Neural style transfer: A review
IEEE transactions on visualization and computer graphics (2019)

[JOS18] JOSANG, A.
Subjective Logic: A formalism for reasoning under uncertainty
Springer, 2018

[KEN17] KENDALL, A., GAL, Y.
What uncertainties do we need in bayesian deep learning for computer vision?
Advances in neural information processing systems, 2017, pp. 5574–5584

[KIN14] KINGMA, D. P., BA, J.
Adam: A method for stochastic optimization
arXiv preprint arXiv:1412.6980 (2014)

[KIN13] KINGMA, D. P., WELLING, M.
Auto-encoding variational bayes
arXiv preprint arXiv:1312.6114 (2013)

[KUR12] KURDEJ, M., MORAS, J., CHERFAOUI, V., BONNIFAIT, P.
Map-aided fusion using evidential grids for mobile perception in urban environment
Belief Functions: Theory and Applications, Springer, 2012, pp. 343–350

[KUZ17] KUZNIETSOV, Y., STUCKLER, J., LEIBE, B.
Semi-supervised deep learning for monocular depth map prediction
Proceedings of the IEEE conference on computer vision and pattern recognition, 2017, pp. 6647–6655

[LAI16] LAINA, I., RUPPRECHT, C., BELAGIANNIS, V., TOMBARI, F., NAVAB, N.
Deeper depth prediction with fully convolutional residual networks
2016 Fourth international conference on 3D vision (3DV), IEEE, 2016, pp. 239–248

[LI15] LI, B., SHEN, C., DAI, Y., VAN DEN HENGEL, A., HE, M.
Depth and surface normal estimation from monocular images using regression on deep features and hierarchical crfs
Proceedings of the IEEE conference on computer vision and pattern recognition, 2015, pp. 1119–1127

[LI14] LI, Q., ZHANG, L., MAO, Q., ZOU, Q., ZHANG, P., FENG, S., OCHIENG, W.

Motion field estimation for a dynamic scene using a 3D LiDAR
Sensors 14.9 (2014), pp. 16672–16691

[LIA18] LIANG, M., YANG, B., WANG, S., URTASUN, R.
Deep continuous fusion for multi-sensor 3d object detection
Proceedings of the European Conference on Computer Vision (ECCV), 2018, pp. 641–656

[LIU15] LIU, F., SHEN, C., LIN, G.
Deep convolutional neural fields for depth estimation from a single image
Proceedings of the IEEE conference on computer vision and pattern recognition, 2015, pp. 5162–5170

[LOM17] LOMBACHER, J., LAUDT, K., HAHN, M., DICKMANN, J., WÖHLER, C.
Semantic radar grids
2017 IEEE Intelligent Vehicles Symposium (IV), IEEE, 2017, pp. 1170–1175

[LON81] LONGUET-HIGGINS, H. C.
A computer algorithm for reconstructing a scene from two projections
Nature 293.5828 (1981), pp. 133–135

[LOO16] LOOP, C., CAI, Q., ORTS-ESCOLANO, S., CHOU, P. A.
A closed-form Bayesian fusion equation using occupancy probabilities
2016 Fourth International Conference on 3D Vision (3DV), IEEE, 2016, pp. 380–388

[LU19] LU, C., MOLENGRAFT, M. J. G. van de, DUBBELMAN, G.
Monocular semantic occupancy grid mapping with convolutional variational encoder–decoder networks
IEEE Robotics and Automation Letters 4.2 (2019), pp. 445–452

[MA20] MA, J., JIANG, X., FAN, A., JIANG, J., YAN, J.
Image matching from handcrafted to deep features: A survey
International Journal of Computer Vision (2020), pp. 1–57

[MAL91] MALLOT, H. A., BÜLTHOFF, H. H., LITTLE, J., BOHRER, S.
Inverse perspective mapping simplifies optical flow computation and obstacle detection
Biological cybernetics 64.3 (1991), pp. 177–185

[MAN20] MANI, K., DAGA, S., GARG, S., NARASIMHAN, S. S., KRISHNA, M., JATAVALLABHULA, K. M.
MonoLayout: Amodal scene layout from a single image
The IEEE Winter Conference on Applications of Computer Vision, 2020, pp. 1689–1697

[MOR11] MORAS, J., CHERFAOUI, V., BONNIFAIT, P.
Moving objects detection by conflict analysis in evidential grids
2011 IEEE Intelligent Vehicles Symposium (IV), IEEE, 2011, pp. 1122–1127

[MOU17] MOUHAGIR, H., CHERFAOUI, V., TALJ, R., AIOUN, F., GUILLEMARD, F.
Using evidential occupancy grid for vehicle trajectory planning under uncertainty with tentacles
2017 IEEE 20th International Conference on Intelligent Transportation Systems (ITSC), IEEE, 2017, pp. 1–7

[NAR18] NARKSRI, P., TAKEUCHI, E., NINOMIYA, Y., MORALES, Y., AKAI, N., KAWAGUCHI, N.
A slope-robust cascaded ground segmentation in 3D point cloud for autonomous vehicles
2018 21st International Conference on intelligent transportation systems (ITSC), IEEE, 2018, pp. 497–504

[ODE16] ODENA, A., DUMOULIN, V., OLAH, C.
Deconvolution and checkerboard artifacts
Distill 1.10 (2016), e3

[OLI16] OLIVEIRA, M., SANTOS, V., SAPPA, A. D., DIAS, P.
Scene representations for autonomous driving: an approach based on polygonal primitives
Robot 2015: Second Iberian Robotics Conference, Springer, 2016, pp. 503–515

[PAG96] PAGAC, D., NEBOT, E. M., DURRANT-WHYTE, H.
An evidential approach to probabilistic map-building
Proceedings of IEEE International Conference on Robotics and Automation, vol. 1, IEEE, 1996, pp. 745–750

[PAN20] PAN, B., SUN, J., LEUNG, H. Y. T., ANDONIAN, A., ZHOU, B.
Cross-view semantic segmentation for sensing surroundings
IEEE Robotics and Automation Letters 5.3 (2020), pp. 4867–4873

[PHI20] PHILION, J., FIDLER, S.
Lift, splat, shoot: Encoding images from arbitrary camera rigs by implicitly unprojecting to 3d
European Conference on Computer Vision, Springer, 2020, pp. 194–210

[PRO19] PROPHET, R., LI, G., STURM, C., VOSSIEK, M.
Semantic Segmentation on Automotive Radar Maps
2019 IEEE Intelligent Vehicles Symposium (IV), IEEE, 2019, pp. 756–763

[PRO18] PROPHET, R., STARK, H., HOFFMANN, M., STURM, C., VOSSIEK, M.
Adaptions for automotive radar based occupancy gridmaps
2018 IEEE MTT-S International Conference on Microwaves for Intelligent Mobility (ICMIM), IEEE, 2018, pp. 1–4

[REI20] REIHER, L., LAMPE, B., ECKSTEIN, L.
A Sim2Real Deep Learning Approach for the Transformation of Images from Multiple Vehicle-Mounted Cameras to a Semantically Segmented Im-

age in Bird's Eye View
arXiv preprint arXiv:2005.04078 (2020)

[REI13] REINEKING, T., CLEMENS, J.
Evidential FastSLAM for grid mapping
Proceedings of the 16th International Conference on Information Fusion, IEEE, 2013, pp. 789–796

[ROD20] RODDICK, T., CIPOLLA, R.
Predicting Semantic Map Representations from Images using Pyramid Occupancy Networks
Proceedings of the IEEE/CVF Conference on Computer Vision and Pattern Recognition, 2020, pp. 11138–11147

[RON15] RONNEBERGER, O., FISCHER, P., BROX, T.
U-net: Convolutional networks for biomedical image segmentation
International Conference on Medical image computing and computer-assisted intervention, Springer, 2015, pp. 234–241

[RUM17] RUMMELHARD, L., PAIGWAR, A., NÈGRE, A., LAUGIER, C.
Ground estimation and point cloud segmentation using SpatioTemporal Conditional Random Field
2017 IEEE Intelligent Vehicles Symposium (IV), IEEE, 2017, pp. 1105–1110

[SAP18] SAPUTRA, M. R. U., MARKHAM, A., TRIGONI, N.
Visual SLAM and structure from motion in dynamic environments: A survey
ACM Computing Surveys (CSUR) 51.2 (2018), pp. 1–36

[SCH18] SCHULTER, S., ZHAI, M., JACOBS, N., CHANDRAKER, M.
Learning to look around objects for top-view representations of outdoor scenes
Proceedings of the European Conference on Computer Vision (ECCV), 2018, pp. 787–802

[SEN18] SENSOY, M., KAPLAN, L., KANDEMIR, M.
Evidential deep learning to quantify classification uncertainty
arXiv preprint arXiv:1806.01768 (2018)

[SHA76] SHAFER, G.
A mathematical theory of evidence
Vol. 42, Princeton university press, 1976

[SHI17] SHI, F., SU, X., QIAN, H., YANG, N., HAN, W.
Research on the fusion of dependent evidence based on rank correlation coefficient
Sensors 17.10 (2017), p. 2362

[SIM14] SIMONYAN, K., ZISSERMAN, A.
Very deep convolutional networks for large-scale image recognition
arXiv preprint arXiv:1409.1556 (2014)

[SLE19] SLESS, L., EL SHLOMO, B., COHEN, G., ORON, S.
Road Scene Understanding by Occupancy Grid Learning from Sparse Radar Clusters using Semantic Segmentation
Proceedings of the IEEE International Conference on Computer Vision Workshops, 2019, pp. 0–0

[SLU19] SLUTSKY, M., DOBKIN, D.
Dual inverse sensor model for radar occupancy grids
2019 IEEE Intelligent Vehicles Symposium (IV), IEEE, 2019, pp. 1760–1767

[SU18] SU, X., LI, L., SHI, F., QIAN, H.
Research on the fusion of dependent evidence based on mutual information
IEEE Access 6 (2018), pp. 71839–71845

[SU15] SU, X., MAHADEVAN, S., XU, P., DENG, Y.
Handling of dependence in Dempster–Shafer theory
International Journal of Intelligent Systems 30.4 (2015), pp. 441–467

[TAN19] TAN, M., LE, Q.
Efficientnet: Rethinking model scaling for convolutional neural networks
International Conference on Machine Learning, PMLR, 2019, pp. 6105–6114

[THR06] THRUN, S., MONTEMERLO, M., DAHLKAMP, H., STAVENS, D., ARON, A., DIEBEL, J., FONG, P., GALE, J., HALPENNY, M., HOFFMANN, G., et al.
Stanley: The robot that won the DARPA Grand Challenge
Journal of field Robotics 23.9 (2006), pp. 661–692

[THR93] THRUN, S. B.
Exploration and model building in mobile robot domains
IEEE international conference on neural networks, IEEE, 1993, pp. 175–180

[TIA20] TIAN, Y., SONG, W., CHEN, L., SUNG, Y., KWAK, J., SUN, S.
Fast planar detection system using a GPU-based 3D Hough transform for LiDAR point clouds
Applied Sciences 10.5 (2020), p. 1744

[UMM17] UMMENHOFER, B., ZHOU, H., UHRIG, J., MAYER, N., ILG, E., DOSOVITSKIY, A., BROX, T.
Demon: Depth and motion network for learning monocular stereo
Proceedings of the IEEE Conference on Computer Vision and Pattern Recognition, 2017, pp. 5038–5047

[VAN95] VAN DAM, J. W., KRÖSE, B. J., GROEN, F. C.
Neural network applications in sensor fusion for an autonomous mobile robot
International Workshop on Reasoning with Uncertainty in Robotics, Springer, 1995, pp. 263–278

[VAS17] VASWANI, A., SHAZEER, N., PARMAR, N., USZKOREIT, J., JONES, L., GOMEZ, A. N., KAISER, ., POLOSUKHIN, I.
Attention is all you need
Advances in neural information processing systems, 2017, pp. 5998–6008

[VEL18] VELAS, M., SPANEL, M., HRADIS, M., HEROUT, A.
Cnn for very fast ground segmentation in velodyne lidar data
2018 IEEE International Conference on Autonomous Robot Systems and Competitions (ICARSC), IEEE, 2018, pp. 97–103

[VER19] VERDOJA, F., LUNDELL, J., KYRKI, V.
Deep Network Uncertainty Maps for Indoor Navigation
2019 IEEE-RAS 19th International Conference on Humanoid Robots (Humanoids), IEEE, 2019, pp. 112–119

[WER15] WERBER, K., RAPP, M., KLAPPSTEIN, J., HAHN, M., DICKMANN, J., DIETMAYER, K., WALDSCHMIDT, C.
Automotive radar gridmap representations
2015 IEEE MTT-S International Conference on Microwaves for Intelligent Mobility (ICMIM), IEEE, 2015, pp. 1–4

[WES19] WESTON, R., CEN, S., NEWMAN, P., POSNER, I.
Probably unknown: Deep inverse sensor modelling radar
2019 International Conference on Robotics and Automation (ICRA), IEEE, 2019, pp. 5446–5452

[WIR18] WIRGES, S., STILLER, C., HARTENBACH, F.
Evidential occupancy grid map augmentation using deep learning
2018 IEEE intelligent vehicles symposium (IV), IEEE, 2018, pp. 668–673

[WU19] WU, Q., LI, H., LI, L., YU, Z.
Quantifying intrinsic uncertainty in classification via deep dirichlet mixture networks
arXiv preprint arXiv:1906.04450 (2019)

[WUL18] WULFF, F., SCHÄUFELE, B., SAWADE, O., BECKER, D., HENKE, B., RADUSCH, I.
Early fusion of camera and lidar for robust road detection based on U-Net FCN
2018 IEEE Intelligent Vehicles Symposium (IV), IEEE, 2018, pp. 1426–1431

[XU17] XU, H., DENG, Y.
Dependent evidence combination based on shearman coefficient and pearson coefficient
IEEE Access 6 (2017), pp. 11634–11640

[YAG87] YAGER, R. R.
On the Dempster-Shafer framework and new combination rules
Information sciences 41.2 (1987), pp. 93–137

[YAG09] YAGER, R. R.
On the fusion of non-independent belief structures
International journal of general systems 38.5 (2009), pp. 505–531

[YAN13] YANG, J.-B., XU, D.-L.
Evidential reasoning rule for evidence combination
Artificial Intelligence 205 (2013), pp. 1–29

[YAN20] YANG, N., STUMBERG, L. v., WANG, R., CREMERS, D.
D3VO: Deep Depth, Deep Pose and Deep Uncertainty for Monocular Visual Odometry
Proceedings of the IEEE/CVF Conference on Computer Vision and Pattern Recognition, 2020, pp. 1281–1292

[YU15] YU, C., CHERFAOUI, V., BONNIFAIT, P.
Evidential occupancy grid mapping with stereo-vision
2015 IEEE Intelligent Vehicles Symposium (IV), IEEE, 2015, pp. 712–717

[ZAD79] ZADEH, L.
On the validity of Dempsters rule of combination, Memo M 79/24
Univ. of California, Berkeley 74 (1979)

[ZHA20] ZHANG, P., TIAN, Y., KANG, B.
A new synthesis combination rule based on evidential correlation coefficient
IEEE Access 8 (2020), pp. 39898–39906

[ZHO17] ZHOU, T., BROWN, M., SNAVELY, N., LOWE, D. G.
Unsupervised learning of depth and ego-motion from video
Proceedings of the IEEE Conference on Computer Vision and Pattern Recognition, 2017, pp. 1851–1858

3 Publications

Bringen wir Vorveröffentlichungen so in die Arbeit rein?

The following earlier publications by the author contain parts of this thesis.

Bibliography of some earlier papers